Interference Voltage Estimation for Implantable Cardiac Pacemaker Electromagnetic Interference at Fourth-Generation (4G) and Fifth-Generation (5G) Sub-6 GHz Cellular Frequency Bands

Shuhei Waki, Takuji Nishikawa, Takashi Hikage, and Manabu Yamamoto

Abstract – Experimental and numerical interference voltage estimations for the active implantable medical device electromagnetic interference due to the state-of-the-art cellular frequency bands are presented. A numerical model of a human torso phantom with a pacemaker was constructed for the finite element method simulation, and the interference voltage characteristics induced at the pacemaker connector at fourth-generation and fifth-generation sub-6 GHz bands were obtained. We confirmed the validity of the numerical results by comparing simulation results and measured interference voltages.

1. Introduction

Wireless devices such as mobile phones and wireless power transfer systems could potentially trigger electromagnetic interference (EMI) on other electronic equipment. The problem of EMI on active implantable medical devices (AIMD; implantable cardiac pacemakers or implantable cardioverter defibrillators) caused by electromagnetic field exposure is the very important [1, 2]. Recently, the fifth-generation (5G) mobile communication system has been widely used in our daily lives. Previously, the EMI on AIMD near a wireless device has been investigated [3], and safety guidelines that specify the distance between an AIMD and a phone device were provided [4]. However, the tissues at radio frequency bands used in fourth-generation (4G) and 5G mobile communication systems need to be sufficiently evaluated. Therefore, we need to establish an EMI assessment method at these frequency bands.

An experimental assessment test for AIMD-EMI is presented in [5]. Because it takes a long time for the test, it is difficult to assess the AIMD-EMI on many types of implantable devices. Moreover, in this testing method, although it is able to investigate whether the AIMD-EMI occurs or does not, the voltage induced at a pacemaker circuit (i.e., the main factor of EMI) is not measured. For these reasons, it is preferable that we more effectively evaluate the AIMD-EMI with a reliable assessment method.

This article proposes the numerical estimation for the AIMD-EMI assessment at 4G and 5G sub-6 GHz cellular frequency bands. We constructed the numerical model of a human torso phantom with a pacemaker and a half-wavelength dipole antenna and performed finite element method (FEM) numerical simulation [6]. Compared with the experimental result, we discuss the validity of the numerical estimation.

2. Estimation of Interference Voltage for AIMD-EMI

In general, AIMD-EMI occurs when the two following situations are satisfied. First, the sensing circuit of the pacemakers detects a signal similar to an electrocardiogram signal or noise. Second, the signal has a higher strength than the sensing threshold level. There are four types of mechanisms that cause these situations: directly conducted current, alternating magnetic field, high-voltage electric field, and an electromagnetic wave. At the radio frequency bands used in mobile communication systems, the main cause of AIMD-EMI is the electric field coupling on the pacemaker connector by the electromagnetic field exposure.

Figure 1 shows the flat human torso phantom for the EMI test and the numerical model. It consisted of an

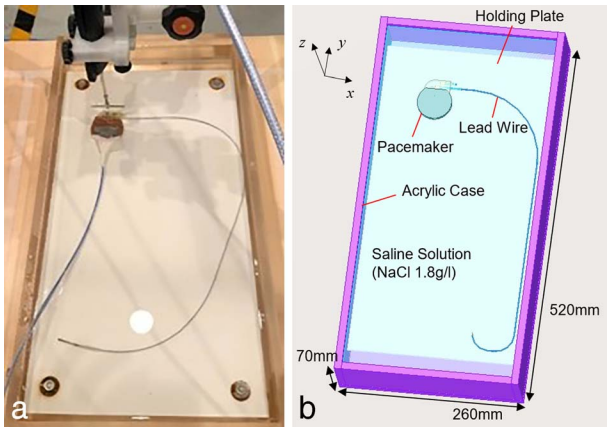

Figure 1. Flat human torso phantom for EMI assessment. (a) Experimental model. (b) Numerical model.

Manuscript received 28 December 2022. This work was supported by Japan Society for the Promotion of Science Grants-in-Aid for Scientific Research (JSPS KAKENHI) Grant Number JP22K04233.

Shuhei Waki, Takuji Nishikawa, Takashi Hikage, and Manabu Yamamoto are with Faculty of Information Science and Technology, Hokkaido University, Kita14, Nishi9, Kita-ku, Sapporo, Hokkaido, 0600814 Japan; e-mail: s_waki@wtemc.ist.hokudai.ac.jp, t_nishikawa@wtemc.ist.hokudai.ac.jp, hikage@wtemc.ist.hokudai.ac.jp, yamamoto@wtemc.ist.hokudai.ac.jp.

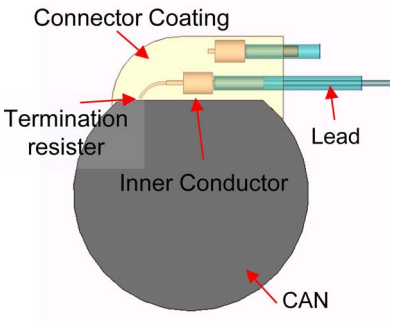

Figure 2. Pacemaker model.

acrylic case and saline solution (NaCl 1.8 g/L). The pacemaker in Figure 2 was placed on the holding panel so that the distance between the pacemaker surface and the phantom surface is 5 mm, as shown in Figure 3a. For this simulation, we constructed numerical models of the half-wavelength dipole antenna operating at 0.8 GHz, 2.0 GHz, 3.7 GHz, and 4.5 GHz to obtain frequency characteristics of interference voltages. The antenna was placed 20 mm from the pacemaker's surface. The antenna input power was normalized to be 1 mW at each frequency. In this simulation, the antenna was shifted in the x-axis direction by 10 mm within a range of ± 60 mm to obtain antenna position dependency of the interference voltages at each frequency, as shown in Figure 3b.

In this study, electromagnetic simulation based on FEM was conducted. Tables 1 and 2 show the analysis condition and the relative permittivity and electrical conductivity of each material used in the human torso phantom. In this article, the voltage induced at the termination resistor (1 MΩ) in Figure 2 was calculated.

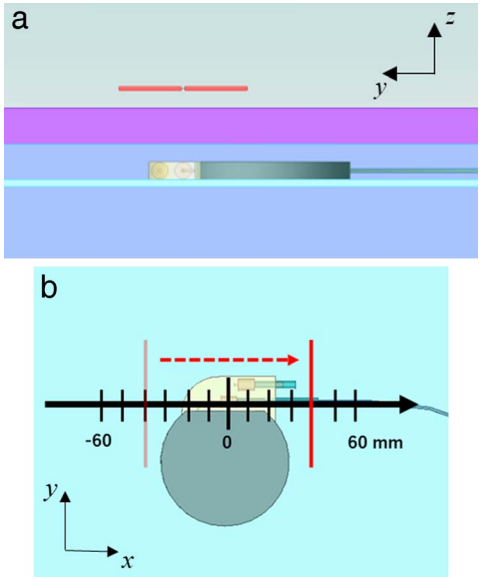

Figure 3. Position of the pacemaker and the antenna. (a) y-z plane. (b) x-y plane.

Table 1. Simulation condition

FEM Solver	Direct Solver
Order of Basis Function	2nd
Boundary Condition	Absorbing
Estimation Frequency	0.8, 2.0, 3.7, 4.5 [GHz]
FEM Mesh	Cond. Edge: 0.05 × estimation conductor width Cond. Vertex: 0.02 × estimation conductor width

We also conducted the measurement with the measurement system in Figure 4. The interference voltage induced at the pacemaker connector can be measured through the electrical-to-optical converter inside the pacemaker can [7]. This article discusses the validity of the numerical simulation with the measurement result.

3. Results and Discussion

Figure 5 shows the simulated and measured interference voltages at each frequency band. The x-axis denotes the antenna position, and the y-axis denotes relative interference voltages normalized by the maximum value obtained at the 0.8 GHz measurement. Each bar denotes measured interference voltages, and each line denotes simulated ones. Both the simulated and measured interference voltage characteristics almost coincide. In the measurements, the maximum interference voltage value at 0.8 GHz (antenna position –20 mm) was approximately 12 dB higher than the one at 4.5 GHz (antenna position –10 mm). The simulated electric field distribution around the pacemaker is shown in Figure 6. Compared with 4.5 GHz, the electric field strength at 0.8 GHz was especially higher at the pacemaker connector, as well as at the lead wire.

Table 2. Dielectric property of materials

Material		ε_r	σ (S/m)
Pacemaker CAN, Lead		Perfect Electric Conductor (P.E.C.)	
Saline Solution (1.8g/l)	0.8 GHz	78.64	0.606
	2.0 GHz	77.76	1.20
	3.7 GHz	76.89	2.97
	4.5 GHz	75.81	4.35
Silicone		2.7	0
Acrylic Case		3	0

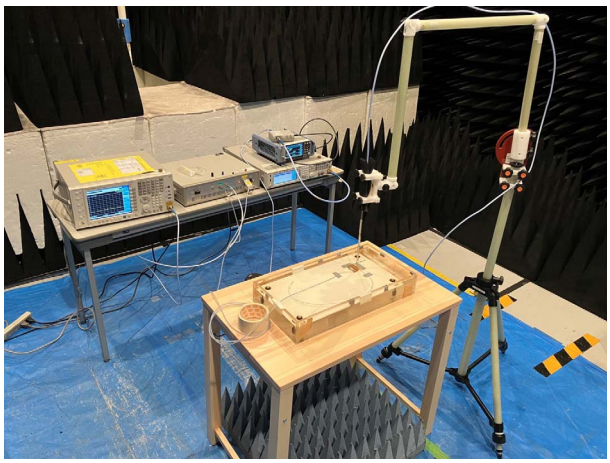

Figure 4. Measurement system.

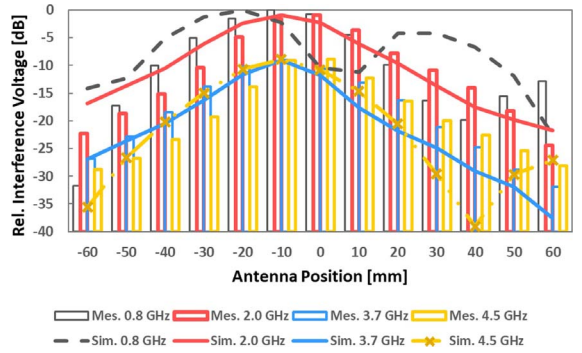

Figure 5. Comparison of simulation results and measurement results (the maximum value in each result is normalized).

This is because the lower the frequency is, the more the radio frequency wave deeply penetrates the saline solution in the phantom, and the electric field coupling at the pacemaker connector becomes dominant. Although a partially large difference in antenna position dependency between simulation and measurement was observed at 0.8 GHz, the numerical results showed a similar tendency to measurements at other frequencies. The difference between the two methods might be attributed to the modeling of the pacemaker circuit and mesh generation in the numerical simulation and the system configuration in the measurement.

4. Conclusion

This article presented numerical simulation for AIMD-EMI assessment at 4G and 5G sub-6 GHz cellular frequency bands. We newly constructed the numerical model of the human torso phantom with the pacemaker and half-wavelength dipole antennas for each frequency band and performed FEM analyses. Compared with the measured results, we confirmed the validity of the simulation. To the best of our knowledge, this is the first article that reports frequency dependency of 4G and 5G cellular bands. The obtained interference voltage characteristics can be contributed to the high reliability and reproductivity of the actual AIMD EMI assessment test. In the future, we will improve the accuracy of the AIMD numerical model, including internal circuits.

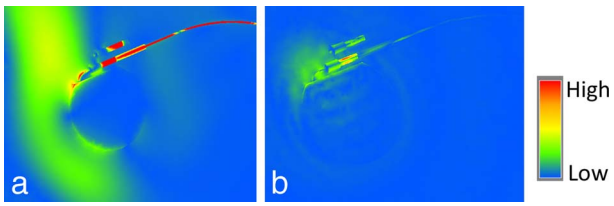

Figure 6. Electric field distribution around the pacemaker.

5. References

1. W. Irnich, L. Bats, R. Muller, and R. Tobisch, "Electromagnetic Interference of Pacemaker by Mobile Phones," *Pacing and Clinical Electrophysiology*, **19**, 10, October 1996, pp. 1431-1446.
2. S. J Seidman, R. Brockman, B. M. Lewis, J. Guag, M. J Shein, et al., "In Vitro Tests Reveal Sample Radiofrequency Identification Readers Inducing Clinically Significant Electromagnetic Interference to Implantable Pacemakers and Implantable Cardioverter-Defibrillators," *Heart Rhythm*, **7**, 1, January 2010, pp. 99-107.
3. T. Hikage, T. Nojima, and H. Fujimoto, "Active Implantable Medical Device EMI Assessment for Wireless Power Transfer Operating in LF and HF Bands," *Physics in Medicine and Biology*, **61**, 12, June 2016, pp. 4522-4536.
4. Ministry of Internal Affairs and Communications, *Guidelines to Prevent Interference on Implantable Medical Devices From Wireless Devices*, Ministry of Internal Affairs and Communications, Tokyo, Japan, August 2005.
5. International Organization for Standardization, *Active Implantable Medical Devices—Electromagnetic Compatibility—EMC Test Protocols for Implantable Cardiac Pacemakers, Implantable Cardioverter Defibrillators, and Cardiac Resynchronization Devices*, ISO 14117:2012, International Organization for Standardization, Geneva, Switzerland, September 2019.
6. Keysight Technologies, *PathWave EM Design 2020*, version, 2020 Update 1, Keysight Technologies, Santa Rosa, CA, USA, https://www.keysight.com/us/en/lib/resources/software-releases/pathwave-em-design-empro-2020.html, 2020.
7. T. Hikage, S. Ito, and A. Ohtsuka, "Novel Interference Voltage Measurement for Beam-Type Wireless Power Transfer Using an Electro-Optical Converter for EMI Assessment of Active Implantable Medical Devices," *URSI Radio Science Letters*, **2**, November 2020, pp. 1-3.